

The Requirement For US28 During Cytomegalovirus Latency Is Independent Of US27 And US29 Gene Expression

Benjamin A. Krishna^{1§}, Amanda B. Wass^{1§}, Rajashri Sridharan¹, Christine M. O'Connor^{1*}

¹Genomic Medicine, Lerner Research Institute, Cleveland Clinic, Cleveland, OH, USA

[§]These authors contributed equally to this work.

* Correspondence:

Christine M. O'Connor, PhD

oconnoc6@ccf.org

Keywords: HCMV, cytomegalovirus, US28, latency, US27.

Abstract

The ability to establish a latent infection with periodic reactivation events ensures herpesviruses, like human cytomegalovirus (HCMV), lifelong infection and serial passage. The host-pathogen relationship throughout HCMV latency is complex, though both cellular and viral factors influence the equilibrium between latent and lytic infection. We and others have shown one of the viral-encoded G protein-coupled receptors, US28, is required for HCMV latency. US28 potentiates signals both constitutively and in response to ligand binding, and we previously showed deletion of the ligand binding domain or mutation of the G protein-coupling domain results in the failure to maintain latency similar to deletion of the entire US28 open reading frame (ORF). Interestingly, a recent publication detailed an altered phenotype from that previously reported, showing US28 is required for viral reactivation rather than latency, suggesting the US28 ORF deletion impacts transcription of the surrounding genes. Here, we show an independently generated US28-stop mutant, like the US28 ORF deletion mutant, fails to maintain latency in hematopoietic cells. Further, we found *US27* and *US29* transcription in each of these mutants was comparable to their expression during wild type infection, suggesting neither US28 mutant alters mRNA levels of the surrounding genes. Finally, infection with a US28 ORF deletion virus expressed US27 protein comparable to its expression following wild type infection. In sum, our new data strongly support previous findings from our lab and others, detailing a requirement for US28 during HCMV latent infection.

1 Introduction

Human cytomegalovirus (HCMV) is a ubiquitous pathogen that latently infects the majority of the population (Khanna and Diamond, 2006). Latent infection in healthy individuals rarely poses a significant health risk, however immune dysregulation can lead to reactivation and CMV-associated disease, which can be fatal (Arvin et al., 2004; Ramanan and Razonable, 2013; Griffiths et al., 2015; Ljungman et al., 2017). This underscores the need to better understand these phases of viral infection to prevent disease and improve patient outcomes.

37 Our current understanding of the biological mechanisms controlling latency and reactivation
38 remain incomplete, though work from many labs have detailed the importance of both host and viral
39 factors in these processes (Collins-McMillen et al., 2018; Elder and Sinclair, 2019). We and others
40 have shown the viral G protein-coupled receptor (GPCR) US28 is required for viral latency (Humby
41 and O'Connor, 2015; Wu and Miller, 2016; Krishna et al., 2017; Krishna et al., 2019). US28 is
42 expressed during both latent and lytic infection (Krishna et al., 2018), and we were the first to detail
43 its requirement for successful HCMV latent infection (Humby and O'Connor, 2015). Building upon
44 our original work, we more recently showed US28 regulates the expression and activity of cellular
45 fos (c-fos) (Krishna et al., 2019), a component of the activator protein-1 (AP-1) transcription factor
46 complex (Halazonetis et al., 1988). US28's attenuation of c-fos leads to a decrease in AP-1 binding
47 to the major immediate early promoter (MIEP) (Krishna et al., 2019), a key regulator in the latent-to-
48 lytic switch (Collins-McMillen et al., 2018). Additionally, our data revealed a requirement for G
49 protein-coupling, and to a lesser extent, ligand binding to US28, suggesting US28-mediated signaling
50 is important for this phenotype (Krishna et al., 2019). This is consistent with findings from the
51 Sinclair Lab, who showed US28 is required for latency in monocytes. Their work also detailed
52 specific signaling pathways US28 impacts to ensure MIEP silencing in these latently-infected cells
53 (Krishna et al., 2017; Elder et al., 2019). Finally, Wu and Miller showed infection of THP-1
54 monocytes with a US28-deletion mutant resulted in robust IE1/2 protein expression, compared to
55 cultures infected with virus expressing US28 (Wu and Miller, 2016). In sum, these data strongly
56 support a significant role for US28-mediated signaling in maintaining a latent infection in
57 hematopoietic cells.

58 Recent work from Crawford et al. challenges these previous findings, as they show US28 is
59 not required for latency, but rather is necessary for reactivation. Using a US28 stop mutant, the
60 investigators demonstrated latency was maintained, but the infection failed to reactivate following the
61 addition of stimuli. Surprisingly, they showed infection with mutant virus containing a point
62 mutation in the ligand binding domain of US28 (Y16F) failed to maintain latent infection, suggesting
63 that while US28 protein (pUS28) expression is not required, ligand binding is essential for latent
64 infection. Crawford et al. suggested a compelling argument that the differences between their work
65 and others were due to the complete ORF deletion of US28 other groups had performed, positing the
66 US28 ORF deletion could impact wild type expression of surrounding genes, namely *US27* and *US29*
67 (Crawford et al., 2019). To date, the impact of the complete US28 ORF on *US27* and *US29* remains
68 unknown.

69 As this is a legitimate concern, we generated an additional set of viral recombinants using an
70 additional BAC-derived clinical isolate, FIX (BFX*wt*-GFP; *wt*). We constructed a triple flag-tagged
71 US28 recombinant (BFX-GFP*inUS28-3xF*; *inUS28-3xF*), from which we then inserted a stop codon
72 immediately following the first methionine (BFX-GFP*stopUS28*; *stopUS28*). Using these
73 independently-generated viruses, we now show, consistent with our previous work (Humby and
74 O'Connor, 2015; Krishna et al., 2019), US28 is dispensable for efficient lytic viral growth in
75 fibroblasts, however this viral GPCR is essential for latency. Our data herein aligns with previous
76 work (Humby and O'Connor, 2015; Wu and Miller, 2016; Krishna et al., 2017; Krishna et al., 2019),
77 as ablation of US28 protein expression in hematopoietic cells that support latency results instead in a
78 lytic-like infection. Additionally, we assessed *US27* and *US29* transcription in both *stopUS28*- and
79 TB40/*EmCherry*-US28 Δ (US28 Δ)-infected fibroblasts, as well as US27 protein (pUS27) in cells
80 infected with a US28 Δ variant and found deletion of the entire open reading frame (ORF) did not
81 impact these transcripts or translation of pUS27 in the absence of US28 expression. Together, our
82 data confirm the requirement for US28 in maintaining HCMV latency, which is independent of *US27*
83 or *US29* mRNA expression.

84 2 Materials and Methods

85 2.1 Cells & Viruses

86 Primary human foreskin fibroblasts (HFF, passages 9 to 13), MRC-5 embryonic lung fibroblasts
87 (MRC-5, passages 21 to 30; ATCC, cat#CCL-171, RRID: CVCL_0440), or newborn human foreskin
88 fibroblasts (NuFF-1, passages 13 to 25; GlobalStem, cat#GSC3002) were maintained in Dulbecco's
89 modified Eagle medium (DMEM), supplemented with 10% fetal bovine serum (FBS), 2 mM L-
90 glutamine, 0.1 mM nonessential amino acids, 10 mM HEPES, and 100 U/ml each of penicillin and
91 streptomycin. Kasumi-3 cells (ATCC CRL-2725, RRID: CVCL_0612) were maintained in RPMI
92 1640 medium (ATCC, cat#30-2001), supplemented with 20% FBS, 100 U/ml each of penicillin and
93 streptomycin, and 100 µg/ml gentamicin at a density of 5×10^5 to 1×10^6 cells/ml. Murine stromal
94 cells S1/S1 and M2-10B4 (MG3) were kind gifts from Terry Fox Laboratories, BC Cancer Agency
95 (Vancouver, BC, Canada). S1/S1 cells were maintained in Iscove's modified Dulbecco's medium
96 (IMDM), supplemented with 10% FBS, 1 mM sodium pyruvate, and 100 U/ml each of penicillin and
97 streptomycin. MG3 cells were maintained in RPMI 1640, supplemented with 10% FBS and 100 U/ml
98 each of penicillin and streptomycin. S1/S1 and MG3 cells were plated in a 1:1 ratio ($\sim 1.5 \times 10^5$ cells
99 of each cell type) onto collagen-coated (1 mg/ml) 6-well plates in human CD34⁺ long-term culture
100 media (hLTCM), containing MyeloCult H5100 (Stem Cell Technologies, cat#5150) supplemented
101 with 1 µM hydrocortisone, and 100 U/ml each of penicillin and streptomycin. The next day, the cells
102 were irradiated using a fixed source ¹³⁷Cesium, Shepherd Mark I Irradiator at 20 Gy, after which the
103 cells were washed three times with 1X PBS, then resuspended in fresh hLTCM and returned to
104 culture. Irradiated murine stromal cells were utilized the following day as feeder cells for the primary
105 CD34⁺ hematopoietic progenitor cells (HPCs). Primary CD34⁺ HPCs were isolated from de-
106 identified cord blood samples (Abraham J. & Phyllis Katz Cord Blood Foundation *d.b.a.* Cleveland
107 Cord Blood Center & Volunteer Donating Communities in Cleveland and Atlanta) by magnetic
108 separation, as described elsewhere (Umashankar and Goodrum, 2014). Isolation and culture methods
109 for the primary CD34⁺ HPCs are detailed below. All cells were maintained at 37°C/5% CO₂.

110 HCMV bacterial artificial chromosome (BAC)-derived strain TB40/E (clone 4) (Sinzger et
111 al., 2008) previously engineered to express mCherry to monitor infection, TB40/*EmCherry*
112 (O'Connor and Shenk, 2011), was used in this study. TB40/*EmCherry*-US28-3xF, TB40/*EmCherry*-
113 US28Δ were previously characterized (Miller et al., 2012). An additional BAC-derived isolate
114 engineered to express eGFP as a marker of infection, BFX_{wt}-GFP (Murphy et al., 2008), was used to
115 generate a recombinant virus expressing a US28 C-terminal triple FLAG epitope tag, BFX_{wt}-GFP-
116 US28-3xF, by bacterial recombineering techniques described in elsewhere (O'Connor and Miller,
117 2014). Briefly, the 3xF epitope and Kan^{frt} cassette were PCR amplified from pGTE-3xFLAG-Kan-
118 frt (O'Connor and Shenk, 2011) using the 3xF-Kan^{frt} insertion primers (Supplementary Table 1).
119 This product was then used to generate BFX-GFP-*in*US28-3xF by recombination (e.g. ref. (O'Connor
120 and Shenk, 2011). BFX_{wt}-GFP-*in*US28-3xF was then used to generate two independent US28 stop
121 mutants using *galk* recombineering, as described previously (O'Connor and Miller, 2014). Briefly,
122 the *galk* gene was amplified by PCR using primers listed in Supplementary Table 1. Recombination-
123 competent SW105 *Escherichia coli* containing BFX-GFP-*in*US28-3xF were transformed with the
124 resulting PCR product. *Galk*-positive clones were selected and electroporated with the double
125 stranded reversion oligonucleotide (Supplementary Table 1) and mutants were counter-selected
126 against *galk*. Two independently generated mutants, BFX-GFP-*stop*US28-S1 and BFX-GFP-
127 *stop*US28-S2, were validated by Sanger sequencing. The multiple epitope tag viral GPCR mutant
128 was generated using TB40/*EmCherry*-US28-3xF as a backbone. Each of the remaining three viral
129 GPCRs were serially epitope tagged with the primers in Supplementary Table 1, and recombinant

130 clones were sequenced following each reversion. The resulting virus, multi-tag vGPCR
131 (vGPCR $_{multi}$), contains the following epitope tags: US28-3xF, US27-3xHA, UL33-c-myc, and
132 UL78-V5. vGPCR $_{multi}$ was then used to generate vGPCR $_{multi}$ -US28 Δ using *galK* recombineering
133 techniques. The primers used to generate this mutant are previously described (Miller et al., 2012).
134 The sequence for vGPCR $_{multi}$ -US28 Δ was verified by Sanger sequencing. All viral stocks were
135 propagated and titered by 50% tissue culture infectious dose (TCID $_{50}$) as described (e.g. ref.
136 (O'Connor and Shenk, 2012).

137 2.2 Viral Growth Analyses

138 Multi-step growth assays were performed using fibroblasts (MRC-5, NuFF-1) by infecting cells at a
139 multiplicity of infection (moi) of 0.01 TCID $_{50}$ /cell. Infectious supernatants were collected over a time
140 course of infection and stored at -80°C until processing. Infectious virus was then titrated on naïve
141 fibroblasts (MRC-5, NuFF-1) and analyzed by TCID $_{50}$ assay.

142 2.3 Viral RNA & Protein Assays

143 For viral transcript analyses, primary NuFF-1 fibroblasts were infected at an moi = 0.5 TCID $_{50}$ /cell.
144 Total RNA was collected 96 hours post-infection (hpi) and RNA was extracted with the High Pure
145 RNA Isolation kit (Roche, cat#11828665001), according to the manufacturer's instructions. cDNA
146 was generated from 1.0 μ g of RNA using TaqMan Reverse Transcription (RT) Reagents and random
147 hexamer primers (Roche, cat#N8080234). Equal volumes of cDNA were used for quantitative PCR
148 (qPCR) using gene specific primers, and cellular *GAPDH* was used as a control (Supplementary
149 Table 1). Transcript abundance was calculated using a standard curve using 10-fold serial dilutions of
150 a BAC-standard that also contains *GAPDH* sequence. Viral gene abundance was normalized to
151 *GAPDH* for each sample. Each primer set had a similar linear range of detection for the BAC-
152 standard (linear between 10⁹ and 10⁴ copies; $r^2 > 0.95$ for all experiments). Samples were analyzed in
153 triplicate using a 96-well format CFX Connect (BioRad).

154 For immunofluorescence assays (IFA), primary MRC-5 or NuFF-1 fibroblasts were grown on
155 coverslips and infected (moi = 0.5) as indicated in the text. Cells were harvested and processed as
156 described elsewhere (e.g. refs. (O'Connor and Shenk, 2011; O'Connor and Murphy, 2012)).
157 Antibodies used include: anti-FLAG M2 (Sigma, cat#F3165, RRID:AB_259529; 1:1,000), anti-HA
158 (Roche, cat#11867423001, RRID:AB_390918; 1:1,000), anti-c-Myc (Sigma, cat#M4439,
159 RRID:AB_439694; 1:500), anti-V5 (Sigma, cat#V8137, RRID:AB_261889; 1:1,000), Alexa 488-
160 conjugated anti-rat (Abcam, cat#ab150157, RRID:AB_2722511; 1:1,000), Alexa 488-conjugated
161 anti-mouse (Fisher, cat#A11001, RRID:AB_2534069; 1:1,000), Alexa 488-conjugated anti-rabbit
162 (Fisher, cat#A11008, RRID:AB_143165; 1:1,000), Alexa 647-conjugated anti-mouse (Abcam,
163 cat#ab150115, RRID:AB_2687948; 1:1,000), 4'-6'-diamidino-2-phenylindole (DAPI). Coverslips
164 were mounted onto slides with Slow-Fade reagent (Invitrogen, cat#S2828) or FluorSave Reagent
165 (Calbiochem, cat#345789), and images were collected using a Zeiss LSM 510 or Leica SP8 confocal
166 microscope.

167 To assess protein expression by immunoblot, $\sim 3.0 \times 10^5$ NuFF-1 fibroblasts were infected
168 (moi = 0.5) for 96h. Cells were harvested in RIPA buffer, and equal amounts of protein were
169 analyzed using the following antibodies: anti-FLAG M2 (Sigma, cat#F3165, RRID:AB_259529;
170 1:7,500), anti-IE1 (clone 1B12 (Zhu et al., 1995); 1:100), anti-pp65 (clone 8A8 (Bechtel and Shenk,
171 2002); 1:100), anti-HA (Roche, cat#11867423001, RRID:AB_390918; 1:1,000), anti-actin (Sigma,
172 cat#A3854, RRID:AB_262011; 1:20,000), and goat-anti-mouse (cat#115-035-003,

173 RRID:AB_10015289) or goat-anti-rat (cat#112-035-003, RRID:AB_2338128) horseradish
174 peroxidase (HRP) secondary (Jackson ImmunoResearch Labs; 1:10,000).

175 **2.4 Latency Infection & Extreme Limiting Dilution Assay**

176 Kasumi-3 cells (moi = 1.0) were infected as described previously (e.g. ref. (Krishna et al., 2019).
177 Briefly, cells were cultured in serum-low media (XVIVO-15; Lonza, cat#04-418Q) for 48h prior to
178 infection. Kasumi-3 cells were infected at a density of 5.0×10^5 cells/ml by centrifugal enhancement.
179 At 7 days post-infection (dpi), cultures were treated with 20nM 12-O-tetradecanoylphorbol-13-
180 acetate (TPA) or vehicle (DMSO) for an additional 2d. Infectious particle production was assessed by
181 Extreme Limiting Dilution Assay (ELDA) on naïve NuFF-1 fibroblasts, as described previously
182 (Umashankar and Goodrum, 2014).

183 Primary CD34⁺ HPC culture and infection conditions are described elsewhere (Umashankar
184 and Goodrum, 2014). Briefly, CD34⁺ HPCs (moi = 2.0) were infected by centrifugal enhancement,
185 followed by overnight incubation. Cells were washed and cultured over irradiated MG3:S1/S1
186 murine stromal cells (plated at 1:1 ratio, see above). At 7 dpi, a portion of each infected cell
187 population was cultured in reactivation media (RPMI 1640, containing 20% FBS, 10 mM HEPES, 1
188 mM sodium pyruvate, 2 mM L-glutamine, 0.1 mM nonessential amino acids, 100 U/ml each
189 penicillin and streptomycin, with 15 ng/ml each (all from R&D Systems): IL-6, G-CSF, GM-CSF,
190 IL-3) or maintained in hLTCM. Infectious particle production was assessed by ELDA on naïve
191 NuFF-1 fibroblasts, as detailed elsewhere (Umashankar and Goodrum, 2014).

192

193 **3 Results**

194 **3.1 *stopUS28* virus replicates to wild type titers in fibroblasts**

195 To ensure US28's function is due to the absence of only this protein as opposed to potential off-site
196 consequences resulting from deletion of the US28 ORF, we generated a new panel of recombinants
197 using the BAC-derived, clinical isolate, BFX_{wt}-GFP (*wt*) (Murphy et al., 2008). The first variant,
198 BFX-GFP_{inUS28-3xF} (*inUS28-3xF*) expresses a pUS28 fusion protein with three, tandem FLAG
199 epitope repeats in the C-terminus of the protein (Fig 1A). Similar to our work in another BAC-
200 derived clinical isolate, TB40/E, in which we made an identical tagged pUS28 recombinant virus
201 (Miller et al., 2012), we observed robust pUS28 expression following lytic infection of fibroblasts by
202 both immunofluorescence assay (IFA; Fig 1B) and immunoblot (Fig 1C). In line with previously
203 published data (Slinger et al., 2010; Noriega et al., 2014), pUS28 localizes to a perinuclear region of
204 infected fibroblasts, consistent with the assembly complex (Silva et al., 2003). Next, we generated
205 two independently derived BFX-GFP_{stopUS28} constructs using the *inUS28-3xF* backbone (Fig 1A),
206 allowing us to confirm protein ablation by both western blot analysis (Fig 1B) and IFA (Fig 1C).
207 Further, consistent with previously published work (Dunn et al., 2003; Yu et al., 2003; Miller et al.,
208 2012; Humby and O'Connor, 2015), we found pUS28 is not required for efficient viral replication in
209 lytically infected fibroblasts, as the two, independently generated stop mutants grew to wild type
210 titers (Supplementary Fig 1). Together, these data confirm pUS28 expression is ablated in *stopUS28*-
211 infected fibroblasts, and pUS28 is dispensable for lytic replication in these cells.

212 **3.2 *stopUS28* fails to maintain latency in hematopoietic cells**

213 We and others have shown deletion of the entire US28 ORF from TB40/E (Humby and
214 O'Connor, 2015; Krishna et al., 2019), Titan (Krishna et al., 2017), and FIX (Wu and Miller, 2016)
215 strains of HCMV results in the failure to establish/maintain latent infection of hematopoietic cells,
216 including Kasumi-3 (Humby and O'Connor, 2015; Krishna et al., 2019) and THP-1 cell lines (Wu
217 and Miller, 2016; Krishna et al., 2017; Krishna et al., 2019), as well as primary monocytes (Krishna
218 et al., 2017) and cord blood-derived CD34⁺ HPCs (Krishna et al., 2019). However, recently published
219 findings reported a US28 stop mutant in TB40/E is capable of maintaining latency in primary fetal
220 liver-derived CD34⁺ HPCs, although this virus failed to reactivate (Crawford et al., 2019). The
221 authors posited that complete ORF deletion possibly impacted efficient expression of surrounding
222 genes, thus potentially contributing to the discrepancies in phenotypes between this and previous
223 studies (Crawford et al., 2019). To determine if our newly generated US28 stop mutant displayed a
224 similar phenotype during latent infection, we infected Kasumi-3 and cord blood-derived CD34⁺ cells
225 with *wt* or *stop*US28 for 7d under latent conditions. We then divided each infected culture, treating
226 half with reactivation stimuli for an additional 2d, where we treated Kasumi-3-infected cultures with
227 TPA and cultured primary CD34⁺ HPCs in reactivation media. We then quantified the production of
228 infectious particles by extreme limiting dilution assay (ELDA) on naïve fibroblasts. *stop*US28-
229 infected cells failed to maintain a latent infection, as Kasumi-3 or CD34⁺ cells infected with this
230 mutant produced infectious virus regardless of reactivation stimuli treatment (Fig 2). These data
231 suggest ablating pUS28 by either introduction of a stop codon or deletion of the ORF results in a
232 variant incapable of maintaining latency in hematopoietic cells.

233 **3.3 Deletion of the US28 ORF does not impact *US27* or *US29* transcription or *US27* protein** 234 **expression**

235 While we observed no difference in the outcome of a US28 stop mutant versus a US28 ORF deletion
236 mutant, we were concerned this mutation may affect neighboring viral transcripts, such as *US27*,
237 which is encoded along with *US28* as a polycistronic transcript (Balazs et al., 2017). Thus, to ensure
238 *US27* and *US29* mRNA expression are unaffected by altered pUS28 expression, we assessed each of
239 these transcripts following lytic infection of fibroblasts with BFX*wt*-GFP or BFX*stop*US28, as well
240 as TB40/*EmCherry* or TB40/*EmCherry*-US28 Δ . We chose to evaluate these transcripts during the
241 lytic life cycle because neither of these genes is expressed during latency (Humby and O'Connor,
242 2015; Cheng et al., 2017; Shnayder et al., 2018). To this end, we lytically infected fibroblasts (moi =
243 0.5), harvested total RNA at 96 hpi, and performed RTqPCR to quantify *US27* and *US29* transcripts,
244 as well as *US28*, *UL123*, and *UL99* as controls. We found ablating pUS28 expression did not impact
245 the transcription of *US27* or *US29* in either US28 recombinant virus (Fig 3). Since *US27* and *US28*
246 originate from a polycistronic RNA, we also assessed US27 protein (pUS27) expression in the
247 context of US28 ORF deletion. To this end, we generated a virus construct in the TB40/*EmCherry*
248 background that contains a different epitope tag on the C-terminus of each viral-encoded GPCR,
249 termed TB40/*EmCherry*-vGPCR*multi* (vGPCR*multi*). Each vGPCR is tagged as follows: US27-
250 3xHA, US28-3xF, UL33-myc, and UL78-V5 (Supplementary Fig 2A). Using this construct, we then
251 generated a US28 deletion, including the triple FLAG epitope tag, termed vGPCR*multi*-US28 Δ
252 (Supplementary Fig 2A), which replicated with wild type kinetics (Supplementary Fig 2B). We then
253 used these newly-generated viral recombinants to lytically infect fibroblasts (moi = 0.5) to determine
254 their localization and expression by IFA and immunoblot, respectively. vGPCR*multi*-infected
255 fibroblasts express each of the four vGPCRs (Supplementary Fig 3), while vGPCR*multi*-US28 Δ fails
256 to express pUS28, as expected (Fig 4). Importantly, complete ORF deletion of US28 does not impact
257 pUS27 expression (Fig 4A) or localization (Fig 4B), consistent with our transcriptional data (Fig 3).
258 Together, these data suggest ablation of pUS28 expression does not impact *US27* and *US29*
259 expression.

260

261 4 Discussion

262 Our findings using newly generated recombinant HCMV constructs reveal pUS28 expression is
263 required for HCMV latency. Our data confirm previous work, wherein we and other groups
264 demonstrated US28 ORF deletion viruses favor lytic rather than latent infection in hematopoietic
265 cells. We now show the insertion of a stop codon after the first methionine in the US28 ORF in the
266 BFX*wt*-GFP background ablates protein expression, which, similar to the US28 ORF deletion virus
267 we previously generated in the TB40/E background, results in a lytic-like infection of both Kasumi-3
268 and cord blood-derived CD34⁺ cells. Our data also suggest *US27* and *US29* gene expression are not
269 impacted by the lack of pUS28 expression, as the US28 stop and deletion viruses express these
270 neighboring transcripts to wild type levels during lytic infection. Furthermore, we show deleting the
271 US28 ORF does not alter the localization or expression of pUS27. Together, our findings support
272 previously published findings detailing the requirement of pUS28 expression for HCMV latency in
273 hematopoietic lineage cells.

274 As mentioned, recent work from Crawford et al. showed the insertion of two tandem stop
275 codons following the first methionine in the US28 ORF resulted in a TB40/E-based mutant capable
276 of maintaining latency, yet incapable of reactivating in response to stimuli. While the US28 stop
277 mutant maintained latent infection, a point mutation (Y16F) within the US28 ligand binding domain
278 failed to do so, leading the authors to conclude that while pUS28 expression was dispensable, ligand
279 binding to pUS28 was required for viral latency (Crawford et al., 2019). Interestingly, mutating the
280 US28 G protein-coupling domain, or the canonical ‘DRY’ motif, which renders US28 “signaling
281 dead” (Waldhoer et al., 2002; Maussang et al., 2006; Maussang et al., 2009; Miller et al., 2012),
282 phenotypically resembled the US28 stop mutant (Crawford et al., 2019). Whether signaling
283 constitutively or in response to ligand binding, a functional G protein-coupling domain is required to
284 potentiate downstream signaling (Haskell et al., 1999; Auger et al., 2002; Schwartz et al., 2006;
285 Rovati et al., 2007). Thus, perhaps in their system, US28 is not behaving as a canonical GPCR. We
286 previously demonstrated a requirement for both US28’s G protein-coupling domain, and to a lesser
287 extent the ligand binding domain, in the context of latent infection. This revealed US28-mediated
288 signaling is required for viral latency and is at least partly dependent upon US28’s interaction with
289 ligand(s) (Krishna et al., 2019). Work from the Sinclair Lab also detailed the requirement for US28’s
290 G protein-coupling domain in suppressing IE protein expression in THP-1 cells, though the Y16F
291 ligand binding mutant suppressed IE protein expression to wild type levels (Krishna et al., 2017). It is
292 important to note we generated a ligand binding mutant, US28 Δ N, in which we deleted amino acids
293 2-16 in the US28 ORF (Krishna et al., 2019), in contrast to the single point mutation, Y16F. We
294 chose to delete these amino acids, as Casarosa et al. previously showed chemokines differentially
295 bind to specific residues within pUS28’s N-terminus (Casarosa et al., 2005). Specific point mutants
296 within this region of pUS28 will undoubtedly prove useful towards identifying the specific ligand(s)
297 with which pUS28 interacts to potentiate latency-specific signaling. Nonetheless, this important
298 variance in the mutants could explain some distinctions between the aforementioned work and ours.

299 What other differences might account for the distinct findings mentioned above? HCMV
300 latency and reactivation are not trivial phases of infection to study in tissue culture. There are various
301 culture systems, viral backgrounds, and culture conditions (e.g. media and additives) that could
302 impact results. We showed pUS28 is required for latency using both the TB40/E (Humby and
303 O’Connor, 2015; Krishna et al., 2019) and BFX*wt* backgrounds, using either ORF deletion (Humby
304 and O’Connor, 2015; Krishna et al., 2019) or stop codon insertion (described herein), respectively.
305 Additionally, Krishna et al published pUS28’s requirement for latent monocyte infection using the

306 Titan strain (Krishna et al., 2017). These consistent findings across strains suggest the viral
307 background most likely does not impact pUS28's requirement for latency. However, conditions used
308 in various latency models may have an impact. A variety of culture systems for the study of latency
309 are characterized (Collins-McMillen et al., 2018; Poole et al., 2019). We use human hematopoietic-
310 derived cells for our experiments (Humby and O'Connor, 2015; Krishna et al., 2019), including the
311 CD34⁺ cell line, Kasumi-3 (O'Connor and Murphy, 2012), THP-1 monocytes (Sinclair et al., 1992),
312 and primary cord blood-derived CD34⁺ hematopoietic cells (Goodrum et al., 2002; Goodrum et al.,
313 2004). Indeed, others have used THP-1 cells (Wu and Miller, 2016; Krishna et al., 2017), as well as
314 primary monocytes (Krishna et al., 2017), to detail pUS28's ability to repress IE gene and protein
315 expression (Wu and Miller, 2016; Krishna et al., 2017), as well as maintain latency (Krishna et al.,
316 2017). The Crawford et al. study used a slightly different model system: CD34⁺ cells derived from
317 fetal liver (Crawford et al., 2019). It is possible, therefore, that while these cells fully support HCMV
318 latency and reactivation, the underlying biological mechanisms the virus uses are distinct from those
319 it employs in cells of hematopoietic origin. It would prove interesting to determine the outcome of
320 infecting the fetal liver-derived CD34⁺ cells with our viral constructs in the future, which may reveal
321 novel differences, while highlighting similarities, with regards to the function of this key protein in
322 different setting.

323 In sum, our work presented herein reveals pUS28 expression is critical to HCMV latency.
324 Further, our data reveal the deletion of the *US28* ORF from our constructs does not impact the
325 expression of the polycistronic transcript, *US27*, or that of the downstream *US29* gene. While we and
326 others have begun to interrogate the signaling pathways pUS28 potentiates to maintain viral latency,
327 further work aimed at understanding the cellular and viral factors pUS28 manipulates during this
328 phase of infection will provide insight into the HCMV-host relationship.

329 **5 Conflict of Interest**

330 The authors declare that the research was conducted in the absence of any commercial or financial
331 relationships that could be construed as a potential conflict of interest. The content is solely the
332 responsibility of the authors and does not necessarily represent the views of the funding institutions.
333 The funding bodies had no role in study design, data collection or interpretation, or the decision to
334 submit the work for publication.

335 **6 Author Contributions**

336 BK, AW, RS, and CO generated reagents and performed experiments. BK, AW, RS, and CO
337 analyzed the data. CO wrote the manuscript. All authors contributed to manuscript revision and
338 approved the submitted version.

339 **7 Funding**

340 This work was supported by Cleveland Clinic funding.

341 **8 Acknowledgments**

342 The authors would like to thank Eain A. Murphy, PhD for critical reading of this manuscript and
343 helpful discussions.

344 **9 References**

- 345 Arvin, A.M., Fast, P., Myers, M., Plotkin, S., Rabinovich, R., and National Vaccine Advisory, C.
346 (2004). Vaccine development to prevent cytomegalovirus disease: report from the National
347 Vaccine Advisory Committee. *Clin Infect Dis* 39(2), 233-239. doi: 10.1086/421999.
- 348 Auger, G.A., Pease, J.E., Shen, X., Xanthou, G., and Barker, M.D. (2002). Alanine scanning
349 mutagenesis of CCR3 reveals that the three intracellular loops are essential for functional
350 receptor expression. *Eur J Immunol* 32(4), 1052-1058. doi: 10.1002/1521-
351 4141(200204)32:4<1052::AID-IMMU1052>3.0.CO;2-L.
- 352 Balazs, Z., Tombacz, D., Szucs, A., Csabai, Z., Megyeri, K., Petrov, A.N., et al. (2017). Long-Read
353 Sequencing of Human Cytomegalovirus Transcriptome Reveals RNA Isoforms Carrying
354 Distinct Coding Potentials. *Sci Rep* 7(1), 15989. doi: 10.1038/s41598-017-16262-z.
- 355 Bechtel, J.T., and Shenk, T. (2002). Human cytomegalovirus UL47 tegument protein functions after
356 entry and before immediate-early gene expression. *J Virol* 76(3), 1043-1050. doi:
357 10.1128/jvi.76.3.1043-1050.2002.
- 358 Casarosa, P., Waldhoer, M., LiWang, P.J., Vischer, H.F., Kledal, T., Timmerman, H., et al. (2005).
359 CC and CX3C chemokines differentially interact with the N terminus of the human
360 cytomegalovirus-encoded US28 receptor. *J Biol Chem* 280(5), 3275-3285. doi:
361 10.1074/jbc.M407536200.
- 362 Cheng, S., Caviness, K., Buehler, J., Smithey, M., Nikolich-Zugich, J., and Goodrum, F. (2017).
363 Transcriptome-wide characterization of human cytomegalovirus in natural infection and
364 experimental latency. *Proc Natl Acad Sci U S A* 114(49), E10586-E10595. doi:
365 10.1073/pnas.1710522114.
- 366 Collins-McMillen, D., Buehler, J., Peppenelli, M., and Goodrum, F. (2018). Molecular Determinants
367 and the Regulation of Human Cytomegalovirus Latency and Reactivation. *Viruses* 10(8). doi:
368 10.3390/v10080444.
- 369 Crawford, L.B., Caposio, P., Kreklywich, C., Pham, A.H., Hancock, M.H., Jones, T.A., et al. (2019).
370 Human Cytomegalovirus US28 Ligand Binding Activity Is Required for Latency in CD34(+)
371 Hematopoietic Progenitor Cells and Humanized NSG Mice. *MBio* 10(4). doi:
372 10.1128/mBio.01889-19.
- 373 Dunn, W., Chou, C., Li, H., Hai, R., Patterson, D., Stolc, V., et al. (2003). Functional profiling of a
374 human cytomegalovirus genome. *Proc Natl Acad Sci U S A* 100(24), 14223-14228. doi:
375 10.1073/pnas.2334032100.
- 376 Elder, E., and Sinclair, J. (2019). HCMV latency: what regulates the regulators? *Med Microbiol*
377 *Immunol* 208(3-4), 431-438. doi: 10.1007/s00430-019-00581-1.
- 378 Elder, E.G., Krishna, B.A., Williamson, J., Lim, E.Y., Poole, E., Sedikides, G.X., et al. (2019).
379 Interferon-Responsive Genes Are Targeted during the Establishment of Human
380 Cytomegalovirus Latency. *MBio* 10(6). doi: 10.1128/mBio.02574-19.
- 381 Goodrum, F., Jordan, C.T., Terhune, S.S., High, K., and Shenk, T. (2004). Differential outcomes of
382 human cytomegalovirus infection in primitive hematopoietic cell subpopulations. *Blood*
383 104(3), 687-695. doi: 10.1182/blood-2003-12-4344.
- 384 Goodrum, F.D., Jordan, C.T., High, K., and Shenk, T. (2002). Human cytomegalovirus gene
385 expression during infection of primary hematopoietic progenitor cells: a model for latency.
386 *Proc Natl Acad Sci U S A* 99(25), 16255-16260. doi: 10.1073/pnas.252630899.
- 387 Griffiths, P., Baraniak, I., and Reeves, M. (2015). The pathogenesis of human cytomegalovirus. *J*
388 *Pathol* 235(2), 288-297. doi: 10.1002/path.4437.
- 389 Halazonetis, T.D., Georgopoulos, K., Greenberg, M.E., and Leder, P. (1988). c-Jun dimerizes with
390 itself and with c-Fos, forming complexes of different DNA binding affinities. *Cell* 55(5), 917-
391 924. doi: 10.1016/0092-8674(88)90147-x.
- 392 Haskell, C.A., Cleary, M.D., and Charo, I.F. (1999). Molecular uncoupling of fractalkine-mediated
393 cell adhesion and signal transduction. Rapid flow arrest of CX3CR1-expressing cells is

- 394 independent of G-protein activation. *J Biol Chem* 274(15), 10053-10058. doi:
395 10.1074/jbc.274.15.10053.
- 396 Humby, M.S., and O'Connor, C.M. (2015). Human Cytomegalovirus US28 Is Important for Latent
397 Infection of Hematopoietic Progenitor Cells. *J Virol* 90(6), 2959-2970. doi:
398 10.1128/JVI.02507-15.
- 399 Khanna, R., and Diamond, D.J. (2006). Human cytomegalovirus vaccine: time to look for alternative
400 options. *Trends Mol Med* 12(1), 26-33. doi: 10.1016/j.molmed.2005.11.006.
- 401 Krishna, B.A., Humby, M.S., Miller, W.E., and O'Connor, C.M. (2019). Human cytomegalovirus G
402 protein-coupled receptor US28 promotes latency by attenuating c-fos. *Proc Natl Acad Sci U S*
403 *A* 116(5), 1755-1764. doi: 10.1073/pnas.1816933116.
- 404 Krishna, B.A., Miller, W.E., and O'Connor, C.M. (2018). US28: HCMV's Swiss Army Knife.
405 *Viruses* 10(8). doi: 10.3390/v10080445.
- 406 Krishna, B.A., Poole, E.L., Jackson, S.E., Smit, M.J., Wills, M.R., and Sinclair, J.H. (2017). Latency-
407 Associated Expression of Human Cytomegalovirus US28 Attenuates Cell Signaling Pathways
408 To Maintain Latent Infection. *MBio* 8(6). doi: 10.1128/mBio.01754-17.
- 409 Ljungman, P., Boeckh, M., Hirsch, H.H., Josephson, F., Lundgren, J., Nichols, G., et al. (2017).
410 Definitions of Cytomegalovirus Infection and Disease in Transplant Patients for Use in
411 Clinical Trials. *Clin Infect Dis* 64(1), 87-91. doi: 10.1093/cid/ciw668.
- 412 Maussang, D., Langemeijer, E., Fitzsimons, C.P., Stigter-van Walsum, M., Dijkman, R., Borg, M.K.,
413 et al. (2009). The human cytomegalovirus-encoded chemokine receptor US28 promotes
414 angiogenesis and tumor formation via cyclooxygenase-2. *Cancer Res* 69(7), 2861-2869. doi:
415 10.1158/0008-5472.CAN-08-2487.
- 416 Maussang, D., Verzijl, D., van Walsum, M., Leurs, R., Holl, J., Pleskoff, O., et al. (2006). Human
417 cytomegalovirus-encoded chemokine receptor US28 promotes tumorigenesis. *Proc Natl Acad*
418 *Sci U S A* 103(35), 13068-13073. doi: 10.1073/pnas.0604433103.
- 419 Miller, W.E., Zagorski, W.A., Brenneman, J.D., Avery, D., Miller, J.L., and O'Connor, C.M. (2012).
420 US28 is a potent activator of phospholipase C during HCMV infection of clinically relevant
421 target cells. *PLoS One* 7(11), e50524. doi: 10.1371/journal.pone.0050524.
- 422 Murphy, E., Vanicek, J., Robins, H., Shenk, T., and Levine, A.J. (2008). Suppression of immediate-
423 early viral gene expression by herpesvirus-coded microRNAs: implications for latency. *Proc*
424 *Natl Acad Sci U S A* 105(14), 5453-5458. doi: 10.1073/pnas.0711910105.
- 425 Noriega, V.M., Gardner, T.J., Redmann, V., Bongers, G., Lira, S.A., and Tortorella, D. (2014).
426 Human cytomegalovirus US28 facilitates cell-to-cell viral dissemination. *Viruses* 6(3), 1202-
427 1218. doi: 10.3390/v6031202.
- 428 O'Connor, C.M., and Miller, W.E. (2014). Methods for studying the function of cytomegalovirus
429 GPCRs. *Methods Mol Biol* 1119, 133-164. doi: 10.1007/978-1-62703-788-4_10.
- 430 O'Connor, C.M., and Murphy, E.A. (2012). A myeloid progenitor cell line capable of supporting
431 human cytomegalovirus latency and reactivation, resulting in infectious progeny. *J Virol*
432 86(18), 9854-9865. doi: 10.1128/JVI.01278-12.
- 433 O'Connor, C.M., and Shenk, T. (2011). Human cytomegalovirus pUS27 G protein-coupled receptor
434 homologue is required for efficient spread by the extracellular route but not for direct cell-to-
435 cell spread. *J Virol* 85(8), 3700-3707. doi: 10.1128/JVI.02442-10.
- 436 O'Connor, C.M., and Shenk, T. (2012). Human cytomegalovirus pUL78 G protein-coupled receptor
437 homologue is required for timely cell entry in epithelial cells but not fibroblasts. *J Virol*
438 86(21), 11425-11433. doi: 10.1128/JVI.05900-11.
- 439 Poole, E., Huang, C.J.Z., Forbester, J., Shnayder, M., Nachshon, A., Kweider, B., et al. (2019). An
440 iPSC-Derived Myeloid Lineage Model of Herpes Virus Latency and Reactivation. *Front*
441 *Microbiol* 10, 2233. doi: 10.3389/fmicb.2019.02233.

- 442 Ramanan, P., and Razonable, R.R. (2013). Cytomegalovirus infections in solid organ transplantation:
443 a review. *Infect Chemother* 45(3), 260-271. doi: 10.3947/ic.2013.45.3.260.
- 444 Rovati, G.E., Capra, V., and Neubig, R.R. (2007). The highly conserved DRY motif of class A G
445 protein-coupled receptors: beyond the ground state. *Mol Pharmacol* 71(4), 959-964. doi:
446 10.1124/mol.106.029470.
- 447 Schwartz, T.W., Frimurer, T.M., Holst, B., Rosenkilde, M.M., and Elling, C.E. (2006). Molecular
448 mechanism of 7TM receptor activation--a global toggle switch model. *Annu Rev Pharmacol*
449 *Toxicol* 46, 481-519. doi: 10.1146/annurev.pharmtox.46.120604.141218.
- 450 Shnayder, M., Nachshon, A., Krishna, B., Poole, E., Boshkov, A., Binyamin, A., et al. (2018).
451 Defining the Transcriptional Landscape during Cytomegalovirus Latency with Single-Cell
452 RNA Sequencing. *MBio* 9(2). doi: 10.1128/mBio.00013-18.
- 453 Silva, M.C., Yu, Q.C., Enquist, L., and Shenk, T. (2003). Human cytomegalovirus UL99-encoded
454 pp28 is required for the cytoplasmic envelopment of tegument-associated capsids. *J Virol*
455 77(19), 10594-10605. doi: 10.1128/jvi.77.19.10594-10605.2003.
- 456 Sinclair, J.H., Baillie, J., Bryant, L.A., Taylor-Wiedeman, J.A., and Sissons, J.G. (1992). Repression
457 of human cytomegalovirus major immediate early gene expression in a monocytic cell line. *J*
458 *Gen Virol* 73 (Pt 2), 433-435. doi: 10.1099/0022-1317-73-2-433.
- 459 Sinzger, C., Hahn, G., Digel, M., Katona, R., Sampaio, K.L., Messerle, M., et al. (2008). Cloning and
460 sequencing of a highly productive, endotheliotropic virus strain derived from human
461 cytomegalovirus TB40/E. *J Gen Virol* 89(Pt 2), 359-368. doi: 10.1099/vir.0.83286-0.
- 462 Slinger, E., Maussang, D., Schreiber, A., Siderius, M., Rahbar, A., Fraile-Ramos, A., et al. (2010).
463 HCMV-encoded chemokine receptor US28 mediates proliferative signaling through the IL-6-
464 STAT3 axis. *Sci Signal* 3(133), ra58. doi: 10.1126/scisignal.2001180.
- 465 Umashankar, M., and Goodrum, F. (2014). Hematopoietic long-term culture (hLTC) for human
466 cytomegalovirus latency and reactivation. *Methods Mol Biol* 1119, 99-112. doi: 10.1007/978-
467 1-62703-788-4_7.
- 468 Waldhoer, M., Kledal, T.N., Farrell, H., and Schwartz, T.W. (2002). Murine cytomegalovirus (CMV)
469 M33 and human CMV US28 receptors exhibit similar constitutive signaling activities. *J Virol*
470 76(16), 8161-8168. doi: 10.1128/jvi.76.16.8161-8168.2002.
- 471 Wu, S.E., and Miller, W.E. (2016). The HCMV US28 vGPCR induces potent Galphaq/PLC-beta
472 signaling in monocytes leading to increased adhesion to endothelial cells. *Virology* 497, 233-
473 243. doi: 10.1016/j.virol.2016.07.025.
- 474 Yu, D., Silva, M.C., and Shenk, T. (2003). Functional map of human cytomegalovirus AD169
475 defined by global mutational analysis. *Proc Natl Acad Sci U S A* 100(21), 12396-12401. doi:
476 10.1073/pnas.1635160100.
- 477 Zhu, H., Shen, Y., and Shenk, T. (1995). Human cytomegalovirus IE1 and IE2 proteins block
478 apoptosis. *J Virol* 69(12), 7960-7970.

479

480 **10 Figure Legends**

481 **Figure 1. US28 protein expression is ablated in *stopUS28*-infected fibroblasts.** (A) BFX_{wt}-GFP
482 (*wt*) was used to generate *inUS28-3xF*, which contains an in-frame triple FLAG epitope tag (3xF) at
483 the C-terminal end of the ORF (checked arrow). *inUS28-3xF* was then used as the template to
484 generate two independent stop mutants, *stopUS28-1* and *stopUS28-2*, that each contains a stop codon
485 following the first methionine (red stop sign). (B,C) Fibroblasts were infected as indicated (moi =

486 0.5). **(B)** Cell lysates were harvested 96 hpi for immunoblot. α -FLAG was used to detect pUS28
487 expression, α -pp65 is a marker of infection, and actin is shown as a loading control. **(C)** Infected
488 cultures were processed for IFA 72hpi. α -FLAG was used to detect pUS28 expression via the 3xF
489 epitope (red). eGFP (green) is a marker of infection, and nuclei were visualized using DAPI (blue).
490 Images were acquired using a 60x objective. **(B,C)** Representative images are shown; n = 3.

491

492 **Figure 2. *stopUS28* fails to maintain latency in hematopoietic cells.** **(A)** Kasumi-3 cells (moi =
493 1.0) or **(B)** CD34⁺ HPCs (moi = 2.0) were infected under latent conditions with the indicated viruses.
494 At 7 dpi, infected **(A)** Kasumi-3 cells were treated with vehicle (DMSO; -TPA, black bars) or TPA
495 (+TPA, gray bars), and **(B)** CD34⁺ HPCs were cultured in hLTCM (pre-reactivation, black bars) or
496 reactivation media (reactivation, gray bars). The fold-change in the frequency of infectious particle
497 production was quantified by ELDA on naïve fibroblasts 14 d later and is graphed relative to WT **(A)**
498 -TPA or **(B)** pre-reactivation. Each data point (circles) is the mean of three technical replicates (i.e.
499 one biological replicate). Error bars indicate standard deviation of three biological replicates.
500 Statistical significance was calculated using two-way ANOVA analyses followed by Tukey's post-
501 hoc analyses. * $p < 0.05$, ** $p < 0.01$, *** $p < 0.001$

502

503 **Figure 3. Abrogating pUS28 expression does not impact *US27* or *US29* transcription.** NuFF-1
504 fibroblasts were infected (moi = 0.5) with **(A)** BFX_{wt}-based or **(B)** TB40/*EmCherry*-based viruses.
505 Total RNA was harvested 96 hpi and *US27*, *US28*, *US29*, *UL123*, and *UL99* mRNA levels were
506 quantified by RTqPCR. Viral gene expression is plotted relative to cellular *GAPDH*. Each data point
507 (circles) is the mean of three technical replicates (e.g. one biological replicate). Error bars indicate
508 standard deviation of three biological replicates, and statistical significance was calculated using two-
509 way ANOVA analyses followed by Tukey's post-hoc analyses. * $p < 0.05$; ns, not significant.

510

511 **Figure 4. *US28* Δ -infected fibroblasts display wild type pUS27 levels.** NuFF-1 fibroblasts were
512 mock-infected (M) or infected with TB40/*EmCherry* (WT), TB40/*EmCherry*-vGPCR_{multi}, or
513 TB40/*EmCherry*-vGPCR_{multi}-*US28* Δ (moi = 0.5). At 96 hpi, **(A)** cell lysates were collected for
514 immunoblot or **(B)** harvested for IFA. **(A,B)** α -FLAG was used to detect US28 via the 3xF epitope,

515 α -HA was used to detect US27 via the 3xHA epitope. **(A)** IE1 is shown as a marker of infection, and
516 cellular actin serves as a loading control. **(B)** US27-3xHA (green), US28-3xF (white), mCherry (red)
517 serves as a marker of infection. DAPI (blue) was used to visualize nuclei. Images were acquired
518 using 40x objective. **(A,B)** Representative images are shown (n = 3).

519

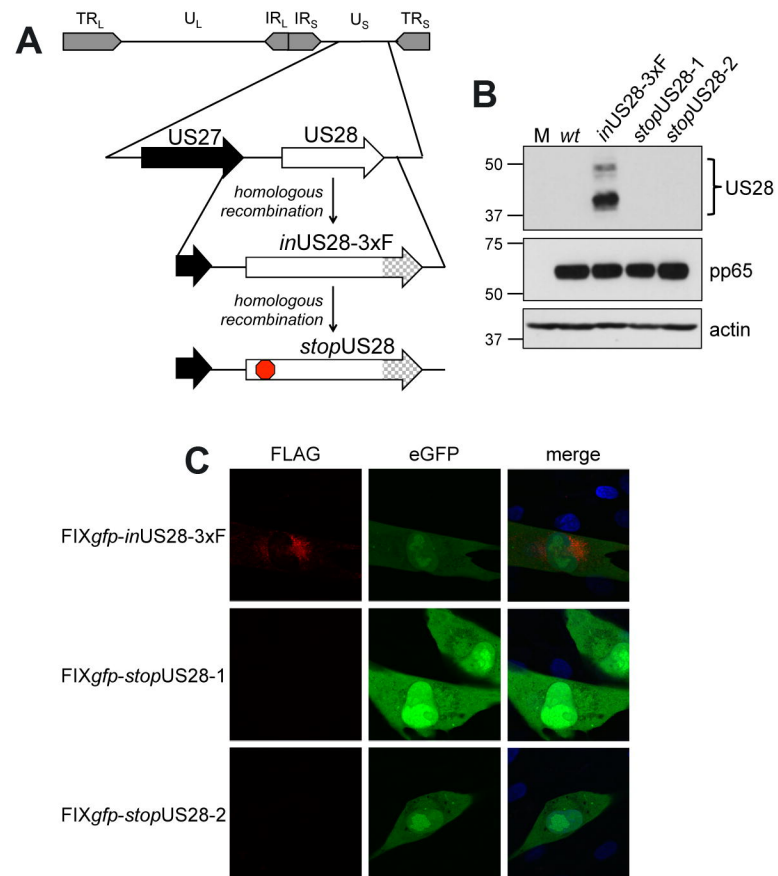


Figure 1. Krishna, et al.

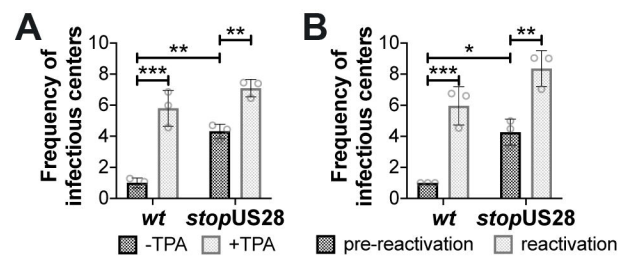


Figure 2. Krishna, et al.

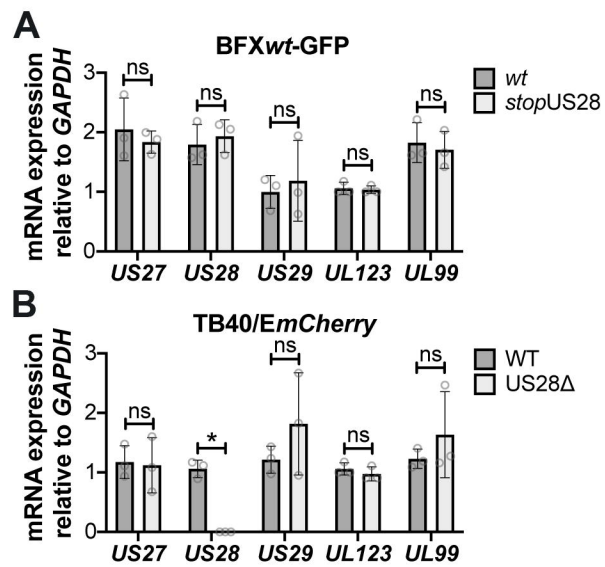


Figure 3. Krishna, et al.

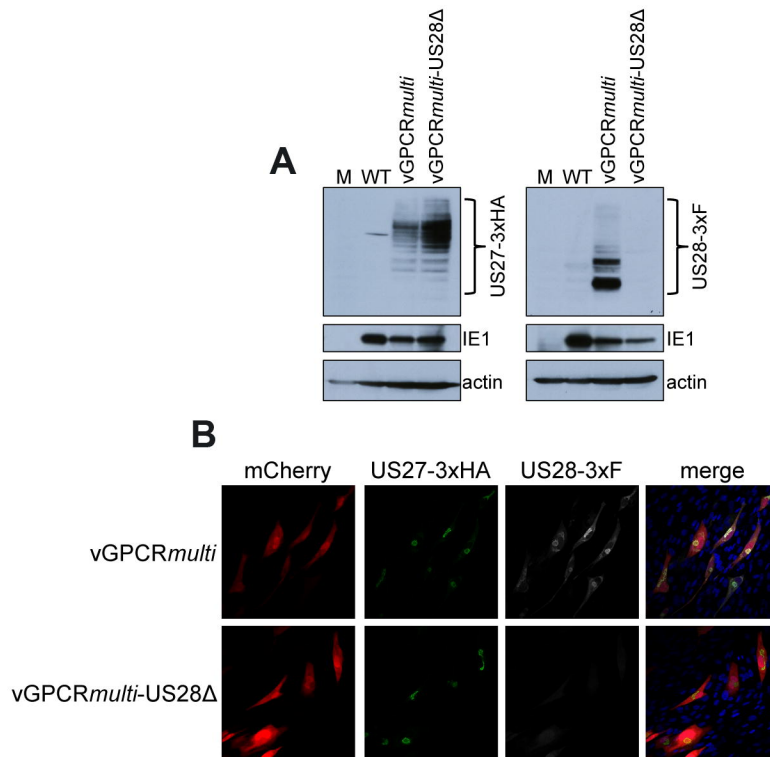


Figure 4. Krishna, et al.